Two-State Thermal Unfolding of a Long Dimeric Coiled-Coil: The *Acanthamoeba* Myosin II Rod

Michal Zolkiewski,*,‡ M. Jolanta Redowicz,§ Edward D. Korn,§ John A. Hammer, III,§ and Ann Ginsburg‡

Section on Protein Chemistry, Laboratory of Biochemistry, and Sections on Cellular Biochemistry and Ultrastructure and on Molecular Cell Biology, Laboratory of Cell Biology, National Heart, Lung and Blood Institute, National Institutes of Health, Bethesda, Maryland 20892

Received December 2, 1996; Revised Manuscript Received April 9, 1997[⊗]

ABSTRACT: *Acanthamoeba* myosin II rod is a long α-helical coiled-coil with a flexible hinge containing a helix-breaking proline. The thermal stability of the complete rod domain of myosin II (residues 849−1509), a mutant in which the hinge proline was replaced by alanine (P398A), and a mutant with the whole hinge region deleted ($\Delta_{384-408}$) was studied in 0.6 and 2.2 M KCl, pH 7.5. In analytical ultracentrifugation studies, the purified myosin II rods sedimented as monodisperse dimers with sedimentation coefficients $s_{20,w} = 3.8$ S (wild-type, $M_r = 149\,000$) and 3.6 S (P398A and $\Delta_{384-408}$). Circular dichroism (CD) and differential scanning calorimetry (DSC) showed that the thermal unfolding of the myosin II rod is reversible and highly cooperative. The unfolding of the rod is coupled to a dissociation of the chains, as shown by HPLC gel filtration at high temperatures and by the concentration dependence of the transition temperature. The CD and DSC data are consistent with a two-state mechanism ($T_m \sim 40$ °C, $\Delta H \sim 400$ kcal/mol) in which the dimeric rod unfolds with concomitant formation of two unfolded monomers. We found no evidence for independent unfolding of the two rod domains that are separated by the hinge region. The only difference observed in the unfolding of the mutant rods from that of the wild type was a ∼2 °C increase in the thermal stability of the hinge-deletion mutant. Thus, the mechanism of unfolding the *Acanthamoeba* myosin II rod is different from those of skeletal muscle myosin rod and tropomyosin, for which non-two-state thermal transitions have been observed. The cooperative unfolding of the entire coiled-coil rod of *Acanthamoeba* myosin II may underlie the previously reported regulatory coupling between its N-terminal head and C-terminal tail.

The coiled-coil structural motif has been found or predicted in numerous proteins, including cytoskeletal and extracellular matrix components, transcription factors, and various cellular and viral surface proteins (Adamson et al., 1993). Coiled-coil sequences contain periodic seven-residue repeats in which the first and fourth positions are occupied by hydrophobic amino acids. Hydrophobic contacts stabilize the structure of a coiled-coil, which is a superhelical complex of α-helices (usually a dimer, although trimers and tetramers have been observed).

The unfolding of short coiled-coils (33−56 amino acids) follows a two-state mechanism (Thompson et al., 1993; Thompson Kenar et al., 1995; Yu et al., 1996). On the other hand, the unfolding of longer coiled-coils (skeletal and smooth muscle myosin rod, tropomyosin) is reported to be a non-two-state reaction (Privalov, 1982; Stafford, 1985; Lopez-Lacomba et al., 1989; Bertazzon & Tsong, 1990; King et al., 1995; O'Brien et al., 1996), although the existence of unfolding intermediates for tropomyosin is controversial (Lehrer & Stafford, 1991). A non-two-state unfolding indicates that the structure of a long coiled-coil is not uniform, but may consist of discrete stable domains each of which unfolds independently of the others. Indeed, the studies of Privalov et al. (1982) on the stability of the skeletal muscle myosin rod showed that the unfolding domains correspond closely to the fragments obtained by limited proteolysis of the rod. It is assumed that the role of local disruptions in a coiled-coil is to provide conformational flexibility (Privalov, 1982). Independent coiled-coil subdomains also may be essential for uncoupling regulatory mechanisms.

Myosin II from *Acanthamoeba castellanii* is a conventional myosin composed of a pair of heavy chains and two pairs of light chains (Maruta & Korn, 1977; Pollard et al., 1978). The *Acanthamoeba* myosin II rod is significantly shorter than that of skeletal muscle myosin (∼90 nm vs ∼160 nm) (Pollard, 1982; McLachlan et al., 1984), but substantially longer than tropomyosin (∼50 nm) (Holtzer et al., 1965). The myosin II rod sequence contains a helix-breaking proline residue at ∼60% of its length (from the N-terminus) (Hammer et al., 1987). Although the sequence of *Acanthamoeba* myosin II is unique among characterized myosins in having a proline located within the α-helical rod, keratin is another coiled-coil protein in which helical segments are separated by proline-containing regions (Letai et al., 1992). The proline position in the myosin II rod corresponds closely to the position of a flexible hinge observed by electron microscopy (Hammer et al., 1987) and also to a trypsin cleavage site (Ganguly et al., 1990). This hinge does not occur in the muscle myosin rod. Another proline is located close to the C-terminus of the *Acanthamoeba* myosin II rod and separates the α-helical coiled-coil from an unstructured

* Address correspondence to this author at the National Institutes of Health, Building 3, Room 212, Bethesda, MD 20892. Fax: (301) 496-0599. E-mail: z5m@cu.nih.gov.
‡ Laboratory of Biochemistry.
§ Laboratory of Cell Biology.
⊗ Abstract published in *Advance ACS Abstracts,* June 1, 1997.

S0006-2960(96)02947-9 This article not subject to U.S. Copyright. Published 1997 by the American Chemical Society

29-residue tail-piece that contains 3 phosphorylation sites/chain (Côté et al., 1984; Hammer et al., 1987). Phosphorylation of these sites inhibits both the actin-activated Mg-ATPase activity of filamentous myosin II (Côté et al., 1981; Collins et al., 1982) and actin filament movement in an in vitro motility assay of filamentous and monomeric myosin II (Ganguly et al., 1992a). Also, phosphorylation of the myosin II carboxyl termini produces conformational changes in the myosin II heads (Ganguly et al., 1992b), and nucleotide binding to the heads affects the conformation of the phosphorylated tail (Redowicz et al., 1994). These results show that communication exists between the N-terminal myosin II heads and C-terminal tails.

This study is part of an effort to determine the significance of the flexible rod hinge in the function and regulation of myosin II. Here, we focused on the stability and the mechanism of unfolding of the myosin II rod. We tested the hypothesis that a hinge in the rod might uncouple the unfolding reactions in the adjacent regions of the coiled-coil structure and thus produce two independent coiled-coil subdomains, as observed by Privalov (1982) for the skeletal muscle myosin rod. We expressed the wild-type myosin II rod, a mutant rod in which the hinge proline was replaced by alanine, and a mutant with the entire hinge region deleted. No deviation from a two-state unfolding was found for the wt[1] or mutant myosin II rods, which indicates the absence of independent cooperative subdomains in this long α-helical coiled-coil.

EXPERIMENTAL PROCEDURES

Proteins. *(A) Expression System.* A 4 kbp genomic DNA corresponding to the entire rod domain (663 amino acid residues) of myosin II from *Acanthamoeba castellanii* was cloned into the *Bam*HI site of the expression plasmid pGEX-KT (Hakes & Dixon, 1992) and expressed in *E. coli* strain HB101 as a GST fusion protein.

(B) Mutagenesis. Site-directed mutagenesis was used to prepare two rod molecules with alterations in the hinge region. In the deletion mutant ($\Delta_{384-408}$), the entire hinge region was removed (residues 384−408) while maintaining the 3/4 periodicity of hydrophobic residues across the deletion. In the point mutant (P398A), the helix breaking proline 398 was changed to alanine. Both mutants were verified by DNA sequencing and expressed as GST fusion proteins exactly as for the wild-type rod.

(C) Purification. Plasmids pGEX-KT containing inserts for expression of appropriate rod preparations were transformed into *E. coli* strain HB101, and expression was induced by adding 0.4 mM IPTG. After ∼3 h, cells were lysed and broken in a French press (lysis buffer: 0.5 M NaCl, 2 mM EDTA, 20 mM imidazole, pH 7.5, 1 mM PMSF, 5 mg/L leupeptin, and 10 mg/L pepstatin; in some preparations, the "Complete" tablets from Boehringer Mannheim were used as a source of protease inhibitors). The lysates were then centrifuged and supernatants were treated with streptomycin, up to 1% (w/v) at pH 7.0, and recentrifuged to remove bulk contamination of nucleic acids. The supernatants were subjected to ammonium sulfate fractionation, up to 65% saturation. Pellets were then dissolved and dialyzed against low-salt buffer containing 20 mM imidazole, 20 mM KCl, and 5 mM Mg^{2+}, pH 7.0, to promote assembly of the GST−rod fusion proteins into filaments. After two cycles of filament assembly−disassembly (alternate dialysis between the above low-salt buffer and 20 mM imidazole, 0.6 M KCl, pH 7.5), the GST−rod fusion proteins were digested with endoproteinase Arg C for ∼14 h at a w/w ratio of 1:30 in order to remove the GST moiety. Proteolysis was terminated with 1 mM PMSF, and digestion mixtures were subjected to another assembly−disassembly cycle. After dialysis against 1 M $(NH_4)_2SO_4$, 0.6 M KCl, and 20 mM imidazole, pH 7.5, the crude rod preparations were loaded onto octyl-Sepharose FF columns. Elution was performed with 0.3 M KCl in 20 mM imidazole, pH 7.5. Fractions containing the rod were collected and concentrated on Centricon 30 (Millipore). Concentrated preparations were stored at 4 °C, and "Complete" tablets were added to prevent proteolysis. Just prior to use, rod preparations were subjected to one cycle of filament assembly−disassembly in order to remove excess protease inhibitors. Purity and integrity of the protein samples were assessed by UV spectrophotometry and polyacrylamide gel electrophoresis in the presence of sodium dodecyl sulfate.

N-Terminal microsequencing of rod preparations, performed by Dr. Brian Martin, confirmed the identity of the rods. Protein concentrations of several purified rod preparations were estimated by amino acid analysis [the myosin II rod has a very low specific absorbance at 280 nm since it contains no Trp and only two Tyr residues/chain (Hammer et al., 1987)]. The CD signal at 222 nm in a 0.2-mm cell was −82.60 for a 1 mg/mL rod solution, and this value was used to calculate the concentrations of other protein stocks.

Circular Dichroism. CD measurements were performed with a Jasco J-710 spectrometer using 0.1- and 0.2-mm water-jacketed cylindrical cells. The temperature of the cell was controlled by an external programmable water bath (Neslab RTE-110). For temperature increases, rates of 7−50 °C/h were used. In a different set of experiments, the temperature was changed stepwise every 1 or 2 °C, and the samples were allowed to equilibrate after each temperature change until time-independent CD signals were obtained. Equilibration times were approximately 30 min for temperature increases with the most concentrated samples and 90 min for temperature decreases with diluted samples.

Differential Scanning Calorimetry. DSC measurements were performed using a Nano-DSC calorimeter (Calorimetry Sciences Corp., Provo, UT). DSC data were corrected for the instrument base line and were normalized for scan rate and protein concentration. Data conversion and analysis were performed using Origin software (MicroCal Inc., Northampton, MA); excess heat capacity was expressed in kcal $(K \cdot mol)^{-1}$, where 1.000 cal = 4.184 J.

Gel Filtration Chromatography. HPLC gel filtration experiments were performed using a Beckman TSK 3000SW column (0.5 mL/min flow rate) and a Hewlett Packard 1090 liquid chromatography system with a temperature-controlled column compartment. To avoid UV absorption due to imidazole, a phosphate running buffer was used. The column was equilibrated at different temperatures for at least 1 h

[1] Abbreviations: wt myosin II rod, an α-helical coiled-coil dimer of the complete rod domain (residues 849−1509) of *Acanthamoeba* myosin II; P398A mutant, myosin II rod with replacement of Pro398 by Ala; $\Delta_{384-408}$ mutant, myosin II rod with deletion of hinge residues 384−408; GST, glutathione *S*-transferase; IPTG, isopropyl β-D-thiogalactopyranoside; PMSF, phenylmethanesulfonyl fluoride; CD, circular dichroism; DSC, differential scanning calorimetry.

before sample injection. The running buffer container and the sample injector were at ambient temperature.

Analytical Ultracentrifugation. The Beckman Optima Model XL-A analytical ultracentrifuge equipped with a four-place AN-Ti rotor was used for sedimentation velocity experiments at 20 °C. The density (ρ) of the dialysate buffer (20 mM K-PO_4, 0.6 M KCl, pH 7.5) at 20.00 ± 0.01 °C was determined to be 1.0308 g/cm^3 with a Paar DMA 58 densitometer, and the relative viscosity (1.024) at 25 °C was measured as described previously (Shapiro & Ginsburg, 1968). Protein samples (0.34 mL) were loaded into the right side of a 4° Kel-F coated double-sector centerpiece, and the reference buffer (0.35 mL) was placed in the left sector in a 12-mm cell. After equilibration at 20 °C at 3000 rpm, the rotor was accelerated to 44 000 or 48 000 rpm, and radial scans of the cells were performed at 230 nm (in the continuous mode with 0.003-cm steps and triple averaging). Sedimentation coefficients (s_{obs}) were calculated using the time-derivative analysis of Stafford (1992), second moment analysis (VELGAMMA), and the radial derivative method (XLAVEL) from Beckman Instruments Inc. Observed sedimentation coefficients were corrected to values corresponding to the viscosity and density of water ($s_{20,w} = 1.118 s_{obs}$). The partial specific volume of the myosin II rod was calculated according to McMeekin and Marshall (1952): $\bar{v} = 0.73$ mL/g. Diffusion coefficients (D) were obtained from the width of a Gaussian fit to the $g(s^*)$ pattern (Stafford, 1996) (see Figure 1B), and solute molecular weights were calculated using the Svedberg equation: $M = RTs/[D(1 - \bar{v}\rho)]$.

Data Analysis for Thermal Unfolding. The CD and DSC data were analyzed using a two-state thermodynamic model in which the unfolding of the rod is coupled to chain dissociation and no intermediate states are populated at equilibrium:

$$F_2 \rightleftarrows 2U \qquad (1)$$

where F is the folded and U is the unfolded myosin II rod chain. The equilibrium constant is defined as $K = U^2/F_2$. If the total monomer (chain) concentration is $c_0 = U + 2F_2$, the fraction of unfolded monomer can be defined as $f_u = U/c_0$, in which case

$$f_u = \frac{\sqrt{K^2 + 8c_0K} - K}{4c_0} \qquad (2)$$

We define a midpoint temperature (T_m), for which $f_u = 0.5$. Therefore, $K(T_m) = c_0$ and $\Delta G(T_m) = \Delta H(T_m) - T_m\Delta S(T_m) = -RT \ln c_0$. If we assume that $\Delta C_p \approx 0$, then for all temperatures $\Delta H = \Delta H(T_m)$, $\Delta S = R \ln c_0 + \Delta H/T_m$, and

$$K(T) = c_0 \exp\left[\frac{\Delta H}{R}\left(\frac{1}{T_m} - \frac{1}{T}\right)\right] \qquad (3)$$

Equation 3 is also adequate for $\Delta C_p \neq 0$ if the data analysis is limited to the vicinity of T_m (Becktel & Schellman, 1987).

Temperature-dependent CD data were described using the equation:

$$CD(T) = (aT + b)(1 - f_u) + (cT + d)f_u \qquad (4)$$

where a, c and b, d are the linear temperature-dependent and temperature-independent contributions, respectively, to the CD signal from the folded (a, b) and unfolded (c, d) protein and f_u is given by eq 2 with K from eq 3. Fitting of eq 4 to the CD data was performed using Origin software. For the analysis of the DSC data, a built-in Origin fitting function was used (with $\Delta C_p \approx 0$), which can be also derived from eqs 2 and 3.

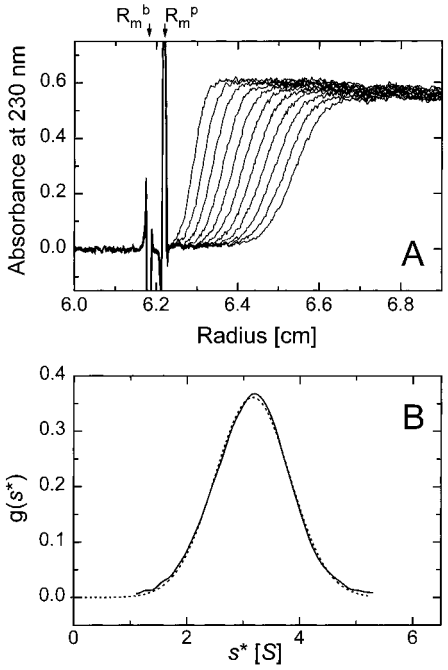

FIGURE 1: Sedimentation velocity experiment at 20 °C for the myosin II rod mutant P398A. (A) Radial scans at 230 nm are shown at 8 min intervals from 24 to 104 min after reaching 48 000 rpm. The direction of sedimentation is to the right, and the radial positions of the buffer meniscus (R_m^b) and the protein solution meniscus (R_m^p) are indicated. (B) Results from time-derivative analysis of Stafford (1992) of four late concentration profiles (see panel A) with a harmonic average sedimentation time of 90 min. The solid line shows an apparent distribution function $g(s^*)$ vs the sedimentation coefficient s^* in Svedberg units (S). The dotted line shows a single Gaussian fit, which indicates a homogeneous, noninteracting solute. The observed sedimentation coefficient of the solute is given by the s^* value at the maximum of the $g(s^*)$ curve.

RESULTS

Homogeneity, Size, and Shape of the Myosin II Rod and Rod Mutants: Ultracentrifugation and Gel Filtration Experiments. Sedimentation velocity experiments were performed to verify the homogeneity of the *Acanthamoeba* myosin II rod samples and to detect possible differences in shape for the wild-type rod and the mutants. A single symmetrical sedimenting boundary was observed for the wild-type rod and both mutants at 20 °C. Figure 1A shows representative scans at 230 nm for the myosin II rod P398A mutant sedimenting at 48 000 rpm. The time derivative of four late concentration profiles for the average time of 90 min (see Figure 1A) is shown in Figure 1B together with the single Gaussian fit of the $g(s^*)$ pattern. The fit of $g(s^*)$ data for the wt and mutant rod samples to a single Gaussian in each case demonstrated the homogeneity of the proteins. The maximum in a $g(s^*)$ plot, such as that shown in Figure 1B, corresponds to s_{obs}, and in all cases this value agreed with sedimentation coefficients calculated from dA/dr vs time and second moment analyses (see Experimental Procedures).

Table 1: Sedimentation Properties of the *Acanthamoeba* Myosin II Rod and Mutant Rods[a]

sample	M_{chain}	c (mg/mL)	$s_{20,w}$ (S)[b]	f/f_0	M_r
wt	74 412	0.075; 0.182	3.81	2.7	151 000
P398A	74 386	0.116	3.58	2.8	145 500
$\Delta_{384-408}$	71 787	0.131	3.56	2.8	143 600

[a] Values are listed for the molecular weights calculated from the amino acid sequence (M_{chain}) and those determined from sedimentation and diffusion coefficients using the Svedberg equation (M_r), protein concentration (c), sedimentation coefficient ($s_{20,w}$) corrected for the density and viscosity of the buffer (see Experimental Procedures), and frictional ratio (f/f_0), where f_0 is the frictional coefficient of a spherical particle with $2M_{chain}$ molecular weight. [b] An accuracy of sedimentation coefficient determinations of ±0.03 S is estimated from two and three separate determinations for wt and mutant myosin II rod samples, respectively.

The results from sedimentation velocity analysis of the myosin II wt rod and the mutants are summarized in Table 1. The molecular weight values calculated from sedimentation and diffusion coefficients indicate that all three proteins are dimers. Small but significant differences in sedimentation coefficients and frictional ratios for the myosin II rod mutants, compared to the wild type (Table 1), have been observed. In several experiments, in which all three rod samples were sedimented simultaneously in the same rotor at the same speed, the mutant rod samples had consistently lower $s_{20,w}$ and higher f/f_0 values than the wt rod. If the shapes of sedimenting rod particles are approximated by those of prolate ellipsoids, the estimated ellipsoid axial ratio is 41 for the wt rod and 45 for the P398A and $\Delta_{384-408}$ rods (Schachman, 1959). Assuming a ~2-nm diameter of a dimeric coiled-coil (Privalov, 1982), the effective length of the myosin II rod ellipsoids is 82 nm for the wt rod and 90 nm for both mutants. The latter value is in agreement with the extended length of the myosin II rod measured by electron microscopy (Hammer et al., 1987) and is close to the value of 94 nm for 632 amino acids in a coiled-coil segment of the full-length myosin II rod and 90 nm for 607 amino acids in $\Delta_{384-408}$, calculated from a 0.148 nm/residue rise of a coiled-coil α-helix (Fraser & Macrae, 1973). The wt ellipsoid is effectively shorter, which is consistent with a bend in the coiled-coil due to the hinge flexibility. As expected, the myosin II rod flexibility was reduced by the hinge mutations. This has been confirmed by electron microscopy (M. J. Redowicz, B. Bowers, E. D. Korn, and J. A. Hammer III, unpublished results) and electric birefringence studies (Redowicz et al., 1996) of the expressed wt and mutant myosin II rods.

In HPLC gel filtration experiments, the native myosin II rod eluted as a single species (Figure 2). When the HPLC column was equilibrated at elevated temperatures, the rod elution volume increased by ~1 mL between 35 and 45 °C, indicating a lower Stokes radius, i.e., an apparently smaller molecule, at the higher temperature. Two distinct molecular species were observed at ~39 °C. The effect of temperature on the behavior of the *Acanthamoeba* myosin II rod was similar to the effect of guanidine hydrochloride on skeletal muscle myosin rod with a ~1 mL increase in elution volume between 1.5 and 2.5 M GdnHCl (Nozais & Bechet, 1993). This elution shift occurred for muscle myosin rod only when the chains of the dimer were not cross-linked and, therefore, could dissociate.[2] The experiment shown in Figure 2 and the concentration dependence of the CD thermal transitions

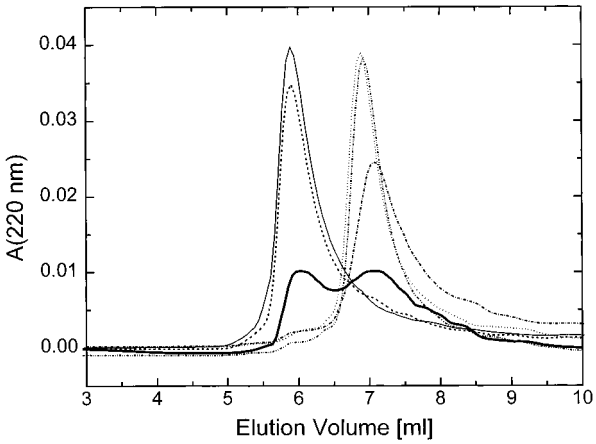

FIGURE 2: Elution profiles of the *Acanthamoeba* myosin II rod (wt) at different temperatures, as determined by HPLC gel filtration. A TSK 3000SW column was equilibrated at 30 °C (—), 35 °C (- - -), 38.5 °C (thick solid line), 39.5 °C (— · —), 45 °C (— ·· —), or 50 °C (···), and 20 μL aliquots of the myosin II rod (0.39 mg/mL) were injected onto the column. The running buffer was 20 mM K-PO_4 and 0.6 M KCl, pH 7.5.

for the *Acanthamoeba* myosin II rod (see below) demonstrate that the rod undergoes a temperature-induced conformational change which is coupled to chain dissociation.

Unfolding Mechanism for the Myosin II Rod and Rod Mutants: CD and DSC Studies. At 25 °C, the myosin II rod had a CD spectrum with negative minima at ~222 and ~209 nm that is characteristic for proteins with predominantly α-helical structure (Figure 3A). At 50 °C, this spectrum changed to that of a random-coil with a minimum at ~204 nm. A complete recovery of the native spectrum was observed after cooling the heated sample and incubating overnight at 25 °C. Thus, the myosin II rod undergoes reversible, thermally induced unfolding. This is similar to unfolding reactions of skeletal and smooth muscle myosin rods (Lopez-Lacomba et al., 1989; Bertazzon & Tsong, 1990; King et al., 1995) and tropomyosin (Lehrer & Stafford, 1991), in which almost complete reversibility of unfolding was observed. In contrast, the thermal unfolding of the whole myosin II is only partially reversible, due to heat-induced aggregation of the myosin II heads (Zolkiewski et al., 1995).

In the initial experiments, the sample temperature was continuously increased at a constant rate, and the CD signal at 222 nm was measured (Figure 3B). The temperature of the thermal transition changed from ~40 to ~42 °C at heating rates of 10 and 50 °C/h, respectively, for the same protein concentration. The complete recovery of the native conformation after heating and cooling the sample showed that no irreversible reactions had taken place, which might have contributed to this apparent kinetic control of unfolding (Freire et al., 1990). Instead, the observed scan-rate dependence of the thermal transition indicates a slow approach to equilibrium, due, most probably, to the dissociation/associa-

[2] In a series of HPLC gel filtration experiments with the skeletal muscle myosin rod under reducing conditions (not shown), we observed an increase in elution volume at elevated temperatures similar to that for the myosin II rod (see Figure 2). This effect was not observed in the absence of a thiol reagent in the running buffer because cross-linking of the myosin rod chains apparently occurred. CD showed a similar loss in secondary structure for reduced and nonreduced skeletal muscle myosin rod at high temperature.

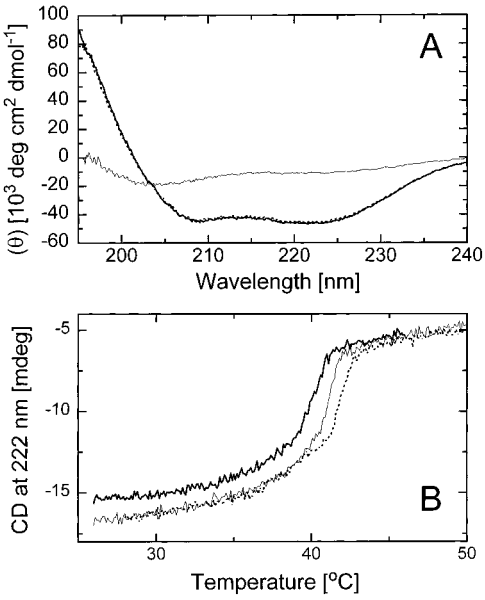

FIGURE 3: (A) Circular dichroism spectra (expressed as mean molar residue ellipticity) of the *Acanthamoeba* myosin II rod (0.86 mg/mL in 10 mM imidazole, 0.6 M KCl, pH 7.5) at 25 °C (solid line), after heating to 50 °C (thin solid line), and after subsequent cooling and incubating overnight at 25 °C (dotted line). (B) Temperature-induced changes in CD at 222 nm for the myosin II rod at different scanning rates: 10 °C/h (thick solid line), 20 °C/h (thin solid line), and 50 °C/h (dotted line).

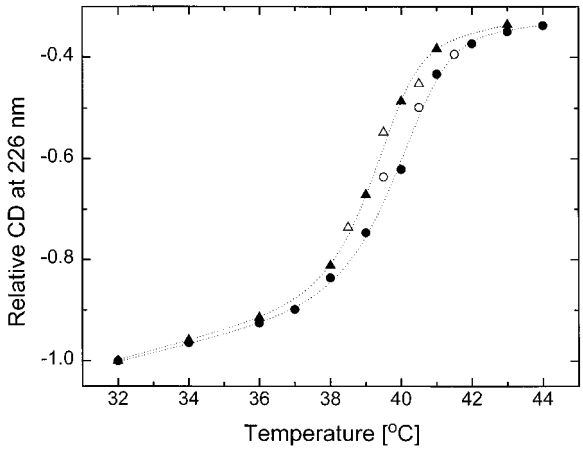

FIGURE 4: Temperature-induced changes in CD at 226 nm for the *Acanthamoeba* myosin II rod (wt) at 0.58 μM (triangles) and 5.75 μM (circles) in 10 mM imidazole, 0.6 M KCl, pH 7.5 (CD normalized to −1.0 at 32 °C). The cell temperature was increased stepwise (filled symbols) and, after reaching the maximum temperature, decreased stepwise (open symbols). The samples were allowed to equilibrate at each temperature until time-independent CD signals were attained (see text for details). Dotted lines show fits of the two-state model with subunit dissociation (eq 4). The refolding data points were not included in the fitting. The parameters of the fit are listed in Table 2 for wild-type and mutant rods.

tion of the two polypeptide chains during the unfolding/refolding reactions.

Figure 4 shows the relative changes in CD at 226 nm for the myosin II rod obtained after equilibration at each indicated temperature (see Experimental Procedures). The CD values measured both for increasing and for decreasing temperatures approximate the calculated curves (see below), which assures that thermodynamic equilibrium had been reached. The thermal transition was concentration-dependent, with transition temperatures different by ~0.8 °C for two samples with 10-fold different concentrations.

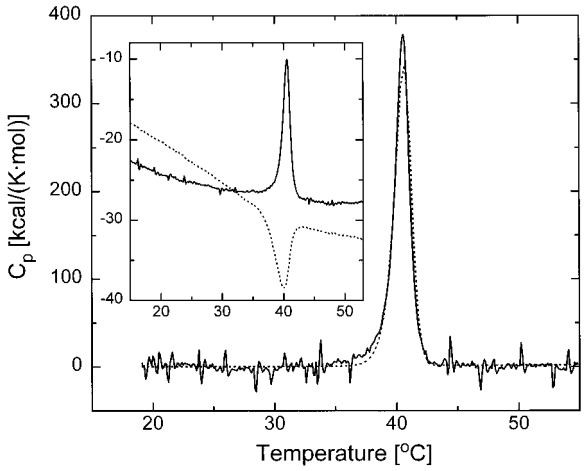

FIGURE 5: DSC scan of the *Acanthamoeba* myosin II rod wt (0.86 mg/mL) at 7.5 °C/h in 10 mM imidazole, 0.6 M KCl, pH 7.5. The instrument base line and a linear base line connecting pre- and posttransition regions were subtracted from the data. The dotted line shows a fit of the two-state model with subunit dissociation. The fitting parameters are given in Table 2 for wild-type and mutant rods. Inset: Experimental DSC data (in μW vs temperature in °C) for the myosin II rod for an up-scan (solid line) and a subsequent down-scan (dotted line) at 7.5 °C/h.

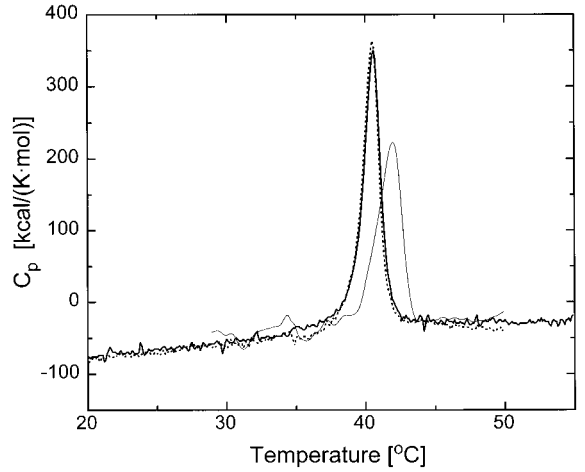

FIGURE 6: DSC of the *Acanthamoeba* myosin II rod and hinge mutants at 7.5 °C/h. The data were corrected for the instrument base line and normalized for protein concentration. Shown are the scans for the wild-type myosin II rod (0.86 mg/mL) (solid line), P398A mutant (0.60 mg/mL) (dotted line), and $\Delta_{384-408}$ mutant (0.23 mg/mL) (thin solid line).

A representative DSC scan at 7.5 °C/h of the wild-type myosin II rod is shown in Figure 5. The midpoint temperature and shape of the DSC transition are similar to the DSC profile obtained previously for the intact myosin II (Zolkiewski et al., 1995). The reversibility of unfolding and the absence of protein aggregates in the rod samples give reliable posttransition base lines, which makes data analysis feasible. The DSC transition for the myosin II rod is asymmetric, a characteristic feature of thermal unfolding curves when subunit dissociation occurs (Freire, 1989). Although it is difficult to obtain a consistent ΔC_p value from several DSC scans (where ΔC_p is a difference between linear low- and high-temperature base lines extrapolated into a transition region), it appears that ΔC_p for the unfolding of wild-type and mutant myosin II rod is $\lesssim$10 kcal/(mol·K) (see raw DSC data in Figure 5, inset, and Figure 6). Differences in shape and transition temperature for the up-scan and down-scan

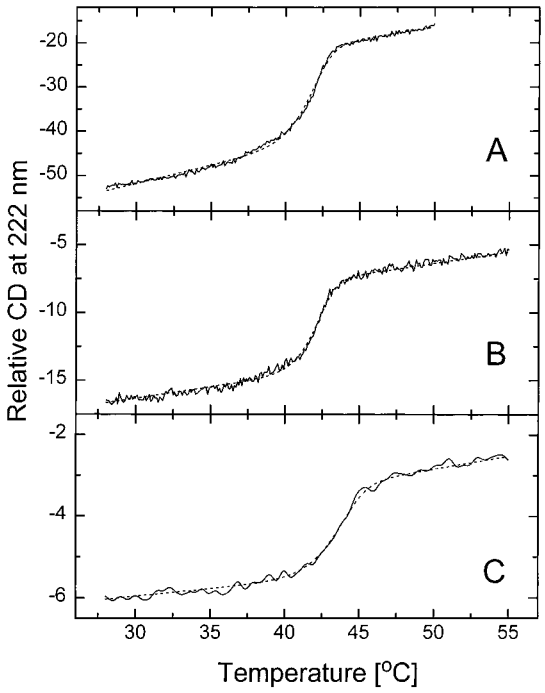

FIGURE 7: Temperature-induced changes in CD at 222 nm for the wild-type *Acanthamoeba* myosin II rod (0.29 mg/mL) (A), P398A mutant (0.19 mg/mL) (B), and $\Delta_{384-408}$ mutant (0.08 mg/mL) (C) at a high ionic strength (10 mM imidazole, 2.2 M KCl, pH 7.5). The temperature was increased with a constant speed of 7 °C/h. The data for the less concentrated $\Delta_{384-408}$ mutant were smoothed using a Fast Fourier Transform. Dotted lines show two-state fits using eq 4. The parameters of the fits are listed in Table 2.

data (Figure 5, inset) suggest different kinetics for the unfolding and refolding reactions of the myosin II rod.

A simple two-state unfolding model which takes into account chain separation (see Experimental Procedures) gives an accurate description of the CD and DSC data (Figures 4, 5, and 7). The parameters of the model (T_m and ΔH) are listed in Table 2. The two-state model predicts a ~1 °C difference in T_m for the two rod concentrations that differ by a factor of 10, which approximates the observed T_m difference of 0.7 °C (Table 2). The assumption of the model ($\Delta C_p \approx 0$) is adequate in the vicinity of T_m since the ΔH values obtained at thermodynamic equilibrium for two different rod concentrations are 410 ± 30 kcal/mol.

Figure 6 compares DSC data for the wild-type myosin II rod and the two mutants with the modified hinge region of the coiled-coil rod. The thermal transitions for both mutants fit a two-state model with chain dissociation. The DSC transition for P398A is identical to that of the wt rod, and $\Delta_{384-408}$ is thermally stabilized with a T_m increase of 1.2 °C (Table 2).

Table 2 contains the unfolding parameters for CD and DSC data obtained under slow scanning conditions as well as at equilibrium. The accuracy of two-state fits for these data is good (see Figures 5 and 7). However, the T_m values for temperature scans are higher by 0.5−0.6 °C than those obtained under equilibrium conditions. The DSC enthalpy values are higher than those obtained from CD measurements at equilibrium. The calculation of thermodynamic parameters from CD requires assumptions about a reaction mechanism, whereas DSC determines directly the enthalpy of reaction. If the protein unfolding equilibrium is coupled to a reaction involving solvent components, the true equilibrium constant is different from that defined by eq 1, and the ΔH values from calorimetry and CD will be different (Naghibi et al., 1995). The unfolding enthalpy for myosin II rod is higher in imidazole than in phosphate buffer[3] (Table 2), which indicates that an exchange of protons between the unfolding rod and buffer components occurs. It can be estimated that the unfolding reaction of the myosin II rod is coupled to a net uptake of ~15 H^+/mol of rod for the wt and P398A and ~8 H^+/mol of rod for $\Delta_{384-408}$. The unfolding enthalpy in a hypothetical buffer with no heat of protonation is 510 kcal/mol for the wt, 520 kcal/mol for P398A, and 460 kcal/mol for $\Delta_{384-408}$. Observe also that ΔH values from CD scans at 7 and 10 °C/h in 0.6 M KCl (Table 2) are higher than those measured under equilibrium conditions, although good two-state fits were obtained for all data sets (compare Figures 4 and 7). This indicates that the slow unfolding kinetics of the myosin II rod affect the shape of the thermal transition at these scanning rates and increase the apparent value of the unfolding enthalpy.

Table 2: Summary of the Thermodynamic Parameters for Unfolding of the *Acanthamoeba* Myosin II Rod and Rod Mutants at pH 7.5 in 10 mM Imidazole Buffer

sample	rod concn (μM)	[KCl] (M)	T_m[a] (°C)	ΔH[b] (kcal/mol)	method
wt	0.58	0.6	39.2	440	CD (equilibrium)
	5.75	0.6	39.9	380	CD (equilibrium)
	5.75	0.6	40.5	640	CD (10 °C/h)
	5.75	0.6	40.5	660	DSC (7.5 °C/h)
	1.1	0.6	40.5[c]	530[c]	DSC (7.5 °C/h)
	1.9	2.2	41.9	380	CD (7 °C/h)
P398A	4.0	0.6	39.9	410	CD (equilibrium)
	4.0	0.6	40.4	510	CD (7 °C/h)
	4.0	0.6	40.4	670	DSC (7.5 °C/h)
	1.2	0.6	40.7[c]	540[c]	DSC (7.5 °C/h)
	1.3	2.2	42.1	400	CD (7 °C/h)
$\Delta_{384-408}$	1.6	0.6	41.3	370	CD (equilibrium)
	1.6	0.6	41.9	450	CD (7 °C/h)
	1.6	0.6	41.7	540	DSC (7.5 °C/h)
	1.0	0.6	42.0[c]	470[c]	DSC (7.5 °C/h)
	0.5	2.2	43.6	290	CD (7 °C/h)

[a] The T_m values are from the fit of the two-state model with subunit dissociation (eq 1). [b] The ΔH values for CD measurements are from the two-state fit, and those for DSC were directly determined by integration of the transition area (see text). [c] The buffer used was 20 mM K-PO_4 (substituted for 10 mM imidazole) and 0.6 M KCl, pH 7.5.

The stability of coiled-coils depends on the ionic strength (Thompson Kenar et al., 1995), and the unfolding mechanism of the skeletal muscle myosin rod can be modified by changing the concentration of chloride ion (Stafford, 1985). We investigated the unfolding transition of the myosin II rod and its mutants at high ionic strength (2.2 M KCl). Under such conditions, all myosin II rod samples were thermally stabilized with T_m increases of 1.4 °C for the wild-type and 1.7 °C for both mutants between 0.6 and 2.2 M KCl (Table 2). No deviations from a two-state unfolding mechanism were observed, however, for wt rod or the P398A and $\Delta_{384-408}$ mutants (Figure 7). This indicates that the absence of populated unfolding intermediates, observed at 0.6 M KCl, applies also at the higher ionic strength.

[3] The enthalpies of buffer protonation at 40 °C are −8.75 kcal/mol for imidazole and −0.15 kcal/mol for phosphate (CRC Handbook of Biochemistry).

DISCUSSION

Although structural domains are not necessarily equivalent to cooperative unfolding units in proteins, such a correspondence has been demonstrated for the long coiled-coil of the skeletal muscle myosin rod (Privalov, 1982). Based on its secondary structure prediction, shape, and proteolysis pattern (Hammer et al., 1987; Ganguly et al., 1990), the *Acanthamoeba* myosin II rod appeared to be a strong candidate for a two-domain protein. It is surprising, therefore, that the whole myosin II rod behaves as a single cooperative thermodynamic domain. Even more striking is the similarity of the unfolding reactions for the wt rod, in which the flexible hinge separates two coiled-coil regions, and the P398A and $\Delta_{384-408}$ mutants, in which the hinge is modified and deleted, respectively. Thus, the existence of flexible regions in a coiled-coil is not necessarily sufficient to establish independent stable subdomains.

It should be recognized, however, that kinetic intermediates can exist in the absence of detectable partially unfolded states at equilibrium. In fact, the slightly higher elution volume for the myosin II rod at 39.5 °C than at 45 and 50 °C (Figure 2) suggests that a protein species migrating differently from a completely unfolded monomer may transiently exist. Unfortunately, the low time-resolution of our CD experiments at different temperatures did not allow an accurate kinetic analysis.

The two *Acanthamoeba* myosin II rod mutants were designed to modify the properties of the flexible hinge in the rod. Analysis of the coiled-coil formation propensity of the wt rod with the PAIRCOIL program (Berger et al., 1995) showed a complete disruption (0 probability) of a coiled-coil at the Pro 398 position with a ~20% decrease in the coiled-coil probability for the rest of the hinge region (residues 380−400). The structure disruption for these residues is much smaller in the P398A mutant, and the $\Delta_{384-408}$ mutant is predicted to form an unperturbed coiled-coil in the region that originally contained the hinge. Relaxation studies using electric birefringence (Redowicz et al., 1996) demonstrated significant differences in flexibility between the wt, P398A, and $\Delta_{384-408}$ myosin II rod minifilaments, as predicted from their differences in sequence. Flexibility differences between the wild type and mutants of the nonfilamentous myosin II rod are also indicated by the length of the rods estimated from sedimentation coefficients reported in this paper and by electron microscopic images (M. J. Redowicz, B. Bowers, E. D. Korn, and J. A. Hammer III, unpublished results).

The two-state thermal unfolding of the myosin II rod according to eq 1 implies that separated chain α-helices are thermodynamically unstable at all temperatures under the buffer conditions used in this study. This unfolding behavior is similar to that of short coiled-coils which contain a leucine zipper motif (Thompson et al., 1993). It can be concluded, therefore, that a major part of the stability of coiled-coils is due to hydrophobic contacts between the chains and not to intrinsic stabilities of the α-helices. Also, each of the two postulated domains in the wt myosin II rod, which are separated by the hinge region, is thermodynamically unstable. The C-terminal domain acquires marginal stability after its isolation by limited proteolysis (Ganguly et al., 1990). Apparently, this stability is not sufficient to populate an intermediate state for the intact rod having a folded C-terminal domain and an unfolded N-terminal domain.

The cooperative unfolding of the whole myosin II rod implies the existence of strong interactions across the hinge, which integrate distant parts of this long coiled-coil into a single cooperative unit. These interactions, which occur with and in spite of significant hinge flexibility, could play an important role in the function of myosin II. Specifically, such interactions may provide a coupling mechanism between regulatory signals which operate at the opposite ends of the myosin II molecule, such as phosphorylation/dephosphorylation of the C-terminal part of the rod and active-site ligand binding in the N-terminal heads (Côté et al., 1981; Collins et al., 1982; Ganguly et al., 1992a,b; Redowicz et al., 1994).

What are the possible reasons for the observed significant qualitative difference between equilibrium unfolding mechanisms for the *Acanthamoeba* myosin II rod and other long coiled-coils? The thermal transition observed in this study for the *Acanthamoeba* myosin II rod is very cooperative (only ~5 °C wide), compared to an ~40 °C wide transition for the skeletal muscle myosin rod (Privalov, 1982; Lopez-Lacomba et al., 1989; Bertazzon & Tsong, 1990). The conflicting reports of two-state unfolding of reduced chicken gizzard tropomyosin (Lehrer & Stafford, 1991) and non-two-state DSC transitions for the same protein (O'Brien et al., 1996) show that the question of a long coiled-coil stability remains a dilemma.

Our results emphasize the importance of making measurements under conditions of thermodynamic equilibrium, the significance of which has frequently been ignored or underestimated in other studies. We found that a 1 °C/min rate of temperature increase, which is used in many unfolding studies, was too fast to allow equilibration of the myosin II rod samples. Although this scanning rate is sufficiently slow for studying unfolding reactions of short coiled-coils (Thompson et al., 1993), it can be expected that slower scanning rates should be used for α-helical rods similar to or longer than the myosin II rod. We did not observe distortions of the unfolding transitions which could produce an appearance of a non-two-state unfolding mechanism (compare Figures 4 and 7) when comparing the CD data for equilibrium and slow scanning conditions. Nonequilibrium conditions do introduce, however, a systematic error in the T_m and ΔH values (see Table 2). Therefore, equilibration of the rod samples was critical for accurate determinations of T_m at different protein concentrations, which is often used as a test for chain dissociation.[4]

A review of the literature on the unfolding of the muscle myosin rod reveals that studies which report two or three apparent two-state transitions (Stafford, 1985; King & Lehrer, 1989; King et al., 1995) used thiol reagents to prevent oxidation of Cys residues, whereas nonreducing conditions were used in DSC studies which report higher numbers of domains (Privalov, 1982; Lopez-Lacomba et al., 1989; Bertazzon & Tsong, 1990). An apparent increase in the cooperativity of unfolding upon inhibition of disulfide formation has been also observed for skeletal muscle myosin subfragment 2 (Lu & Lehrer, 1984). The *Acanthamoeba*

[4] The CD thermal transitions for two samples of myosin II rod with 100-fold different concentrations appeared to have the same T_m when a scanning rate of 10 °C/h was used (compare to equilibrium conditions shown in Figure 4).

myosin II rod does not contain Cys residues, and its two-state thermal unfolding is coupled to chain separation (Figures 2 and 4). Thus, in order to determine rigorously the unfolding mechanisms of other long coiled-coils, it is necessary to detect possible interchain cross-links between α-helices and to determine whether thermal reactions cause chain dissociation for each coiled-coil.

ACKNOWLEDGMENT

We thank Dr. Brian Martin for performing N-terminal microsequencing of the myosin II rod preparations and Dr. James Sellers for the coiled-coil probability analysis for the myosin II rod with the PAIRCOIL program of Berger et al. (1995).

REFERENCES

Adamson, J. G., Zhou, N. E., & Hodges, R. S. (1993) *Curr. Opin. Biotechnol. 4*, 428−437.
Becktel, W. J., & Schellman, J. A. (1987) *Biopolymers, 26*, 1859−1877.
Berger, B., Wilson, D. B., Wolf, E., Tonchev, T., Milla, M., & Kim, P. S. (1995) *Proc. Natl. Acad. Sci. U.S.A. 92*, 8259−8263.
Bertazzon, A., & Tsong, T. Y. (1990) *Biochemistry 29*, 6453−6459.
Collins, J. H., Côté, G. P., & Korn, E. D. (1982) *J. Biol. Chem. 257*, 4529−4534.
Côté, G. P., Collins, J. H., & Korn, E. D. (1981) *J. Biol. Chem. 256*, 12811−12816.
Côté, G. P., Robinson, E. A., Appella, E., & Korn, E. D. (1984) *J. Biol. Chem. 259*, 12781−12787.
Fraser, R. D. B., & Macrae, T. P. (1973) *Conformation in Fibrous Proteins*, Academic Press, New York.
Freire, E. (1989) *Comments Mol. Cell. Biophys. 6*, 123−140.
Freire, E., van Osdol, W. W., Mayorga, O. L., & Sanchez-Ruiz, J. M. (1990) *Annu. Rev. Biophys. Biophys. Chem. 19*, 159−188.
Ganguly, C., Atkinson, M. A. L., Attri, A. K., Sathyamoorthy, V., Bowers, B., & Korn, E. D. (1990) *J. Biol. Chem. 265*, 9993−9998.
Ganguly, C., Baines, I. C., Korn, E. D., & Sellers, J. (1992a) *J. Biol. Chem. 267*, 20900−20904.
Ganguly, C., Martin, B., Bubb, M., & Korn, E. D. (1992b) *J. Biol. Chem. 267*, 20905−20908.
Hakes, D. J., & Dixon, J. E. (1992) *Anal. Biochem. 202*, 293−298.
Hammer, J. A. III, Bowers, B., Paterson, B. M., & Korn, E. D. (1987) *J. Cell Biol. 105*, 913−925.
Holtzer, A., Clark, R., & Lowey, S. (1965) *Biochemistry 4*, 2401−2411.
King, L., & Lehrer, S. S. (1989) *Biochemistry 28*, 3498−3502.
King, L., Seidel, J. C., & Lehrer, S. S. (1995) *Biochemistry 34*, 6770−6774.
Lehrer, S. S., & Stafford, W. F., III (1991) *Biochemistry 30*, 5682−5688.
Letai, A., Coulombe, P. A., & Fuchs, E. (1992) *J. Cell Biol. 116*, 1181−1195.
Lopez-Lacomba, J. L., Guzman, M., Cortijo, M., Mateo, P. L., Aguirre, R., Harvey, S. C., & Cheung, H. C. (1989) *Biopolymers 28*, 2143−2159.
Lu, R. C., & Lehrer, S. S. (1984) *Biochemistry 23*, 5975−5981.
Maruta, H., & Korn, E. D. (1977) *J. Biol. Chem. 252*, 6501−6509.
McLachlan, A. D. (1984) *Annu. Rev. Biophys. Bioeng. 13*, 167−189.
McMeekin, T. L., & Marshall, K. (1952) *Science 116*, 142−143.
Naghibi, H., Tamura, A., & Sturtevant, J. M. (1995) *Proc. Natl. Acad. Sci. U.S.A. 92*, 5597−5599.
Nozais, M., & Bechet, J. J. (1993) *Eur. J. Biochem. 218*, 1049−1055.
O'Brien, R., Sturtevant, J. M., Wrabl, J., Holtzer, M. E., & Holtzer, A. (1996) *Biophys. J. 70*, 2403−2407.
Pollard, T. D. (1982) *J. Cell Biol. 95*, 816−825.
Pollard, T. D., Stafford, W. F., III, & Porter, R. M. E. (1978) *J. Biol. Chem. 253*, 4798−4808.
Privalov, P. L. (1982) *Adv. Protein Chem. 35*, 1−104.
Redowicz, M. J., Martin, B., Zolkiewski, M., Ginsburg, A., & Korn, E. D. (1994) *J. Biol. Chem. 269*, 13558−13563.
Redowicz, M. J., Rau, D. C., Korn, E. D., & Hammer, J. A. III (1996) *Biophys. J. 70*, A160.
Schachman, H. K. (1959) *Ultracentrifugation in Biochemistry*, p 239, Academic Press, New York.
Shapiro, B. M., & Ginsburg, A. (1968) *Biochemistry 7*, 2153−2167.
Stafford, W. F., III (1985) *Biochemistry 24*, 3314−3321.
Stafford, W. F., III (1992) *Anal. Biochem. 203*, 295−301.
Stafford, W. F., III (1996) *Biophys. J. 70*, A231.
Thompson, K. S., Vinson, C. R., & Freire, E. (1993) *Biochemistry 32*, 5491−5496.
Thompson Kenar, K., Garcia-Moreno, B., & Freire, E. (1995) *Protein Sci. 4*, 1934−1938.
Yu, Y., Monera, O. D., Hodges, R. S., & Privalov, P. L. (1996) *Biophys. Chem. 59*, 299−314.
Zolkiewski, M., Redowicz, M. J., Korn, E. D., & Ginsburg, A. (1995) *Arch. Biochem. Biophys. 318*, 207−214.

BI962947C